



Agent-Based Modelling and Simulation of Airport Terminal Operations Under COVID-19-Related Restrictions

Gregory Sanders, S. Sahand Mohammadi Ziabari^(✉) , Adin Mekić, and Alexei Sharpanskykh 

Delft University of Technology, Delft, The Netherlands
{A.Mekic, O.A.Sharpanskykh}@tudelft.nl

Abstract. The worldwide COVID-19 pandemic has had a tremendous impact on the aviation industry, with a reduction in passenger demand never seen before. To minimize the spread of the virus and to gain trust from the public in the airport operations' safety, airports implemented measures, e.g., physical distancing, entry/exit temperature screening and more. However, airports do not know what the impact of these measures will be on the operations' performance and the passengers' safety when passenger demand increases back. The goal of this research is twofold. Firstly, to analyze the impact of current (COVID-19) and future pandemic-related measures on airport terminal operations. Secondly, to identify plans that airport management agents can take to control passengers' flow in a safe, efficient, secure and resilient way. To model and simulate airport operations, an agent-based model was developed. The proposed model covers the main airport's handling processes and simulates local interactions, such as physical distancing between passengers. The obtained results show that COVID-19 measures can significantly affect the passenger throughput of the handling processes and the average time passengers are in contact with each other. For instance, a 20% increase in check-in time (due to additional COVID-19 related paperwork at the check-in desk) can decrease passenger throughput by 16% and increase the time that passengers are in contact by 23%.

Keywords: Multi-agent system · Airport operations · COVID-19 · Physical distancing · Walking behavior

1 Introduction

The outbreak of the COVID-19 pandemic has led to a worldwide crisis and presents us today unprecedented challenges in our life. The aviation industry has been impacted like no other industrial sector. When in March 2020 large clusters of COVID-19 cases were identified in Europe, many countries started to impose travel restrictions. As a result, the travel demand dropped and global air traffic decreased by 80% compared to the preceding year [1]. The aviation industry has never faced a challenge this large. To minimize the spread of the COVID-19 virus and regain the public's trust in the aviation industry's safety, airports needed to be made safe. Since at airports passengers are

often exposed to many interactions with other people, airport operators implemented measures. Some examples of measures are physical distancing, entry/exit temperature screening, prevention of queuing, use of personal protective equipment. To help airports implement measures, the European Aviation Safety Agency released in June 2020 their “COVID-19 Aviation Health Safety Protocol” [2]. This report lists measures that airport operators can take for safe operations to guarantee the passengers’ safety. These measures, for instance social distancing, are widely considered as a new part of our life. These recommended measures from EASA already helped many airports in providing safe operations. However, many airports still do not know the impact of these measures on their operations when passenger demand will increase. For example, Charleroi Airport faced a sudden increase in passenger demand during the Christmas Holiday of 2020. As a result, the airport was too crowded and passengers could not perform physical distancing [3]. Also, airports are very complex because they involve many processes (e.g., check-in, security, boarding) and many stakeholders (airlines, airport operators), resulting in conflicting objectives. On the one hand, airports operators have the financial intent to increase revenue and decrease costs. On the other hand, they also need to make sure that operations are safe for the passengers. While airports are now under financial pressure, it is hard for them to make decisions primarily since they do not understand the impact of these measures. To address this problem agent-based modelling and simulation was used in this research. These emergent properties can be translated into system-wide key performance indicators (KPIs), for example passenger throughput, and can be used to assess, e.g., the system’s performance and safety. Altogether, agent-based modelling is a suitable paradigm to model airport terminal operations.

This paper is organized as follows. In Sect. 2 the related work is discussed. The agent-based model is discussed in Sect. 3. The different case studies and the results are given in Sect. 4. Finally, Sect. 5 is Discussion and Conclusion.

2 Related Work

Related works should at least cover two main categories namely, different pedestrian dynamics models to simulate passenger walking behavior, and pandemic modeling and analysis. We will briefly go through each of them.

In general pedestrian dynamics models can be categorized into microscopic models and macroscopic models [4]. In microscopic models, every pedestrian is treated as an individual unit and is given a certain amount of characteristics, for instance direction and speed. The changes in movement of each pedestrian is influenced by other pedestrians and by the environment. Gips et al. proposed the benefit-cost cellular model for modelling pedestrian flows [5]. Blue et al. proposed cellular automata microsimulation for modeling bi-directional pedestrian walkways [6]. These two models are cellular automata-based models which means that the environment of the model is discretized in a grid. The downside of this type of models is that the simulation does not reflect the real behavior of pedestrians because updates in the grid are done heuristically [4, 7]. The queuing network model was introduced in [8]. In this model the environment is discretized into links and nodes. Pedestrians move from one node to another node. The movement is stochastic because it uses Monte Carlo simulations. This model has several drawbacks. Firstly, movement is unidimensional and therefore it is not so realistic

because pedestrians walk bi-dimensional. Secondly, the model cannot not deal with high density environments, like airport terminals. Thirdly, because of the discretized environment, the model lacks the ability to analyze local interactions between the different agents. Okazaki introduced a magnetic force model for pedestrian movement simulation with evacuation and queueing [9]. This model is based on the magnetic field theory to simulate pedestrian movement. Helbing et al. came up with the social force model [10]. The social-force model uses psychological forces that drive pedestrians to move towards their goal as well as keep a proper distance from other pedestrians and objects. The values of the parameters of the social forces have a physical meaning and therefore calibrating these parameters for social distancing is easier.

The second category investigates the studies which used agent-based models to analyze the impact of COVID-19 on the performance of airport terminal operations and on the associated passenger health safety. Kierzkowski et al. uses a discrete event simulation model for different security lane configurations to analyze the impact of social distancing on the performance of the security [11]. However, this model lacks the ability to model local interactions between passengers because it is a discrete event simulation model. Furthermore, they only evaluate the performance of the security lanes and not the associated health safety of the passengers. Schultz et al. used a cellular automata model to simulate different aircraft boarding strategies under COVID-19 related restrictions [12]. He assessed for each boarding strategy the impact on total boarding time, the feasibility of the procedure and the associated risk of virus transmission. Schultz et al. used a transmission model which was based on the work of [13]. The study of Schultz et al. lacks to analysis of other processes and activities at the airport such as check-in or security. Ronchi et al. developed a model-agnostic approach to perform a quantitative assessment of pedestrian exposure using the outputs of existing microscopic crowd models, namely the trajectories of pedestrians over time [14]. The model uses a general formulation instead of relying on a specific disease transmission. For instance, the quantification of the pedestrian exposure is based on the distances between pedestrians, the time pedestrians are exposed and reference points (e.g. pedestrian face each other). It is therefore universal and can be tailored to new pandemics when there is no compelling understanding in the transmission of the pandemic.

3 The Agent-Based Model

The model used in this paper is an extension of the baseline “Airport And Terminal Operations Model” (AATOM) with features to simulate passengers adhering to COVID-19 measures and to analyze passengers health safety [15]. In this model, passengers and airport operators are represented as autonomous intelligent entities, called agents. These agents are modelled with a particular behavior approximating humans and placed in a partially observable airport environment. An overview of the agent-based system is provided in Fig. 1.

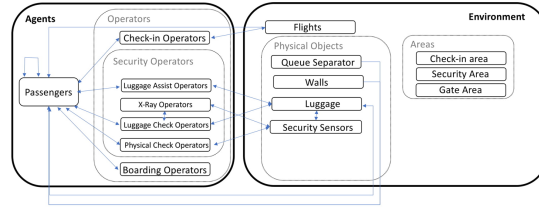


Fig. 1. Overview of the multi-agent system including the different types of agents and their interactions with each other and the environment.

3.1 Specification of the Environment, and the Agents

The model’s environment represents an airport terminal under COVID-19 conditions, as seen in Fig. 2. It resembles an existing regional airport from the Netherlands. The environment consists of three main areas: the check-in area, the security checkpoint area and the gate area. The check-in area consists of four sets of check-in desks, each with three desks and one designated queue. There is a check-in operator (red dot), which checks-in passengers, behind each check-in desk. Three check-ins are using a common zig-zag queue. One check-in is using three single straight queues. There are four types of security operators (A, B, C, D) as indicated in the lower part of Fig. 2. Operators A assist passengers in their luggage drop activity. Operators B perform the x-ray scan activity. Operators C perform the luggage check-activity and operators D perform a physical check when a passenger is suspicious. The black dots represent the luggage divest and luggage collect positions. Figure 2 shows three divest and three collect positions per lane, respectively. The number of divest and collect positions can vary depending on the input to the model. The model contains three types of agents: passenger agents adhering to COVID-19 rules, passenger agents not adhering to COVID-19 rules and operator agents. These three types all share the AATOM cognitive architecture described by [15] and shown in Fig. 3. The shaded blocks of Fig. 3 show the extensions and improvements made to the baseline AATOM model. The security checkpoint area consists of four security lanes and one large common queue. The checkpoint lanes have a luggage belt, an X-ray sensor and a walk-through metal detector.

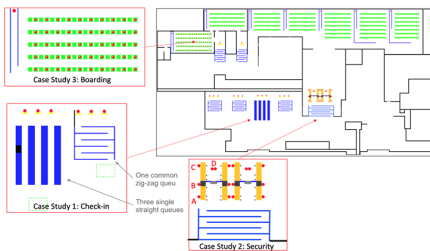


Fig. 2. The environment of the agent-based model. (Color figure online)

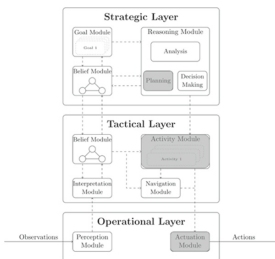


Fig. 3. Cognitive architecture of AATOM.

3.2 Specification of the Interactions Between Passenger Agents

Physical distancing has an impact on the interaction between passengers. For this study, the movement module and the activity module of the baseline AATOM model were revised to include physical distancing between the agents when they are walking and when they are queuing. The Helbing social force model handles the movement of passenger agents [10]. It is performed in the actuation module of the cognitive architecture presented in Fig. 3. The model assumes that the passengers' movement is guided by a superposition of attractive and repulsive forces, determining the passengers' walking behavior. The pushing force and a friction force refer to the forces when passengers collide with each other. These forces are not important for the model because passengers are not allowed to touch each other; they need to keep their distance. The social repulsion force $f_{social\ rep}$, on the other hand, is important for simulating physical distancing. The social repulsion force $\vec{f}_{social\ rep}$ is modelled by Eq. 1 and was calibrated in order to simulate physical distancing between the agents. It models the psychological tendency of two pedestrians i and j to stay away from each other. r_{ij} is the sum of the radii of pedestrian i with radius r_i and pedestrian j with radius r_j . d_{ij} is the absolute distance between the pedestrians i and j (taken from their center of mass). \vec{n}_{ij} is the normalized vector from pedestrian j to i and is calculated by: $\vec{n}_{ij} = (n_{ij}^1, n_{ij}^2) = (\vec{r}_i - \vec{r}_j)/d_{ij}$. A_i and B_i are the "Helbing" constants [10]. These Helbing constants define the distance between passengers and are therefore crucial in modelling physical distancing.

$$\vec{f}_{social\ rep} = A_i e^{(r_{ij}-d_{ij})/B_i} \vec{n}_{ij} \quad (1)$$

In the baseline AATOM model, no difference was made between the social repulsion force of two agents and the social repulsion force of an agent and an object. The values of A and B for both scenarios were taken 250 [N] and 0.1 [m], respectively. The values of A and B for both scenarios were taken 250 [N] and 0.1 [m], respectively. However, in the model for this research study, the distinction is made between both. In this model, every passenger agent that performs physical distancing is given two sets of Helbing parameters. One set of parameters to simulate the social repulsion force of a passenger agent with the environment. Another set of parameters to simulate the social repulsion force of a passenger agent with other passenger agents. For the first set, the values of A and B were taken to be equal to the original values 250 [N] and 0.1 [m] such that emergence of the interactions is similar to the baseline AATOM model. For the second set, the B value was calibrated to represent physical distancing between agents. In Fig. 4 one can see the impact of parameter B on the social repulsion force. The higher the B value, the earlier the social repulsion force is activated. The B was increased to 0.5 m (while A remains 250 [N]). It was visually inspected by simulation that a B value 0.5 m guarantees a physical distancing between passengers while still representing correct walking behavior.

The agent-based model is able to identify at each time point which passenger agents are not performing physical distancing, this will be referred to as using "agents that are in contact". One analyzer was implemented in the model that represents the number of passengers that are in contact at every time step. This is shown in Fig. 5(a). This analyzer is used to determine the contact locations. A second analyzer, presented in Fig. 5(b),



Fig. 4. Plot of social repulsion force $f_{\text{social repulsion}}$ [N] vs distance between the passengers d_{ij} [m]. The blue graph is the social repulsion force of the baseline AATOM model (when agents are not physically distancing). The orange graph is the social repulsion force for the extended AATOM model where agents are physically distancing. (Color figure online)

integrates the first and represents the total time of all passengers that were in contact. This analyzer is used as a metric for results of the case studies presented in Sect. 4. A third analyzer, in Fig. 5(c), shows the summed contact time but with a distinction between ‘face-to-face’ contacts and ‘everything-back contacts’.

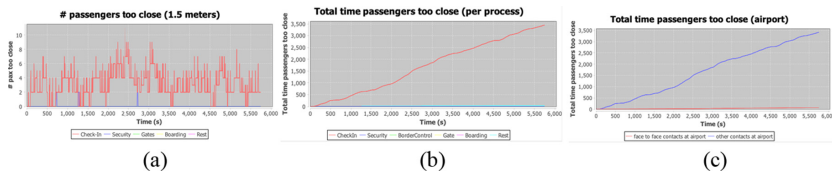


Fig. 5. The passenger contact analyzers. (a) Analyzer showing the amount of agents that are in contact at every time step and at which location. Case study 1: scenario 5. (b) Analyzer showing summed time of all passengers that were in contact. The amount of contacts (figure on the left) are integrated over time. Case study 1: scenario 5. (c) Analyzer showing summed time of all passengers that were in contact. Case study 1: scenario 5.

4 Case Studies

For this research, three different case studies are performed. The check-in process is analyzed in Sect. 4.1. The security process is analyzed in Sect. 4.2 and finally, the boarding process is analyzed in Sect. 4.3. In each case study, different hypotheses are answered by simulating various scenarios in which different COVID-19 measures are modelled. Every scenario is simulated 450 times. These three case studies all share a common goal: they aim to analyze the impact of the COVID-19 measures on the performance of the process and the passengers’ health safety. The model set-up and the used metrics are explained in the following three sections.

4.1 Case Study 1: Check-In

In this case study only the check-in is considered, as presented in Fig. 2. This case study aims to analyze the impact of three COVID-19 measures: Firstly, the impact of physical distancing between passengers. Secondly, the impact of longer waiting times at the desk due to additional paperwork related to COVID-19. Thirdly, the impact of a different queue lay out, for instance three straight queues instead of one common zig-zag queue. The following three metrics are developed to analyze the effect of these measures on the system's performance and the associated health safety of the passengers: 1. Check-in throughput T_C , calculated in passengers per hour. Check-in throughput is defined as the number of passengers that were served by a check-in area in a specific time period. Note a check-in area consists out of three check-in desks. 2. Average contact time per passenger C_{pax} , calculated in seconds. Contact time per passenger is defined as the time duration for which a passenger agent is not able to perform at least 1.5 m physical distancing. For the check-in case study, two variants of this metric were designed. Namely, A) the average contact time per passenger in the check-in queue C_{paxCQ} . This metric only considers the contact time of a passenger for which the passenger was in the queue during the check-in process. B) The average contact time per passenger at the check-in desk C_{paxCD} . This metric is thus only calculated for the passengers that are at the desk. These two variants were implemented to understand at which location the passenger is exposed the most: in the queue or at the desk. Using these metrics, five different hypotheses were found to be the most interesting to analyze:

- **Hypothesis 1:** Physical distancing decreases check-in throughput T_C .
- **Hypothesis 2:** Physical distancing decreases average contact time per passenger in the queue C_{paxCQ} .
- **Hypothesis 3:** A 20% increase in check-in time t_{Ci} increases the average contact time per passenger in the queue C_{paxCQ} .
- **Hypothesis 4:** Three single straight queues (instead of one common zig-zag queue) result in a higher check-in throughput T_C .
- **Hypothesis 5:** Three single straight queues (instead of one common zig-zag queue) result in a lower average contact time per passenger C_{paxCQ} .

These four hypotheses are tested by simulating five different scenarios. Passenger agents are generated in front of check-in queue and they only perform the check-in activity and the queue activity. The inputs to the model for each scenario are given in Table 1. Scenario 1 models a pre-COVID-19 situation. No COVID-19 measures are modelled in this scenario. Thus, passenger agents do not perform physical distancing. No extra paperwork is required. Therefore, the check-in time t_{Ci} follows a normal distribution with a mean of 60 min and a variance of 6 min. This is based on data that is gathered before COVID-19 [16, 17]. Passenger agents are using a common zig-zag queue. In scenario 2, the 1.5-m physical distancing measure is modelled. Scenario 1 and 2 are used to test hypotheses 1 and 2. In scenario 3, a 20% increase in check-in time t_{Ci} is modelled, thus $N(72,6)$, in order to account for additional health questions and more paperwork related to COVID-19. This scenario is used to test hypothesis 3. In scenario 4, the measures of scenario 2 and 3 are modelled together. Lastly, in scenario 5 passenger

agents use a straight check-in queue instead of a common zig-zag queue. This scenario is used to test hypotheses 4 and 5.

Results for Check-In

Table 1 presents the results of the check-in case study, Sect. 4.1. For hypothesis 1, Table 1 shows that scenario 1 and 2 result in the same check-in throughput T_C , namely 167 passengers per hour. This means that physical distancing PD does not influence the check-in throughput T_C . This was confirmed by the coefficient of correlation $\rho_{PD, T_C} = -0.11$ with $p\text{-value} = 0$. Since the $\rho_{PD, T_C} < 0.4$ (rule of thumb) we can say there is no significant correlation between these two variables. Thus, we can reject hypothesis 1. For hypothesis 2, Table 1 shows that in scenario 1 a passenger is on average 4 s in contact at the desk C_{paxCD} and 1 min and 25 s in contact with other passengers in the queue C_{paxCQ} . For scenario 2, C_{paxCD} is the same but C_{paxCQ} reduced with 41%. This means that physical distancing does decrease C_{paxCQ} . This is confirmed by the strong negative correlation coefficient: $\rho_{PD, C_{paxCQ}} = -0.9$ with $p\text{-value} = 0$. Therefore, we can support hypothesis 2. For hypothesis 3, it can be deduced from scenario 3 in Table 1 that an extra 20% more check-in time t_{ci} (due to e.g., extra COVID-19 related paper work) increases the average contact time per passenger in the queue C_{paxCQ} by 23%. The coefficient of correlation $\rho_{t_{ci}, C_{paxCQ}} = +0.72$ with $p = 0$. This means there is a significant positive correlation between t_{ci} and C_{paxCQ} . Therefore, we can support hypothesis 3. This is reasonable because t_{ci} also reduces the check-in throughput T_C with 16% which results in longer waiting times for passengers in the queue. For hypothesis 4 and 5, three single queues were implemented in scenario 5 instead of one common zig-zag queue. Table 1 reveals that straight queues increase passenger throughput with a small 3%. The coefficient of correlation ρ_{QT, T_C} equals 0.24, which is lower than 0.4, meaning there is no significant correlation. We can reject hypothesis 4. The introduction of three single queues also reduced C_{paxCD} by 50% and C_{paxCQ} by 42%. The coefficients of correlation $\rho_{QT, C_{paxCD}}$ and $\rho_{QT, C_{paxCQ}}$ are -0.86 and -0.74 . This confirms that single queues reduce the average contact time per passenger C_{pax} . Hypothesis 5 can be supported. The reason for this reduction is threefold: 1. Due to the three straight queues, the passenger flow from the end of the queue towards the check-in desk is more efficient. Fewer passengers interfere with each other because there are three queue exits instead of one. 2. The absence of corners in a straight queue. Figure 6 shows that in a zig-zag most contacts occur in the corners (dark blue dots). In a straight queue, Passengers do not need to turn while queuing. When passengers are turning, they focus less on other passengers than when they walk in a straight line. 3. The model implementation: a passenger agent is programmed to stop when observing other passenger agents that are in queueing mode and are at 1.5 m distance. At corners, the passenger's observation can be blocked by a wall which causes that other passenger agents are observed too late (when the passengers are already closer than 1.5 m).

4.2 Case Study 2: Security Check Point

Case study 2 only considers the security process. This case study's environment is the security checkpoint area, as shown in Fig. 2. This case study aims to analyze the impact of the COVID-19 measures on the performance of the security checkpoints and the

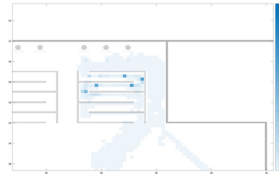


Fig. 6. Heatmap scenario 2. The dark blue areas represent the hot spots of passenger contacts. (Color figure online)

Table 1. Results of case study 1: check-in. PD means physical distancing, t_{ci} means time to check-in. Note that percentages are given w.r.t. the baseline scenario 1. For every scenario 450 simulations were performed.

Check-in scenario	Input to Model		T_C			$C_{pax_{CD}}$			$C_{pax_{CQ}}$		
	Queue Type	PD	t_{ci} [sec]	μ [pax/h]	σ^2 [pax ² /h ²]	μ [min:sec]	σ^2 [sec ²]	μ [min:sec]	σ^2 [sec ²]	%	
1	One common	No	N(60,6)	167	0.3136	00:04	0.0410	01:25			
2	One common	Yes	N(60,6)	167	0.3548	00:04	0.0365	00:50	-41%	3.1109	
3	One common	No	N(72,6)	140	0.4750	00:04	0.0334	01:45	23%	1.9986	
4	One common	Yes	N(72,6)	140	0.6131	00:04	0.0337	01:03	-26%	6.2027	
5	Three single	Yes	N(72,6)	145	0.3422	00:02	0.0194	00:27	-68%	23.773	

associated passenger health safety. Similar metrics as for the check-in case study are used, namely: 1. Average security throughput T_S , calculated in passengers per hour. Security throughput is defined as the number of passengers that were served by two security lanes in a specific time period. 2. Average contact time per passenger C_{pax} , calculated in seconds. Two variants of this metric were designed to identify at which location most contacts occur. Namely, A) the average contact time per passenger in the security queue $C_{pax_{SQ}}$. B) The average contact time per passenger at the security lane $C_{pax_{SL}}$. Also, for this case study some hypotheses were found interesting to be analyzed:

- **Hypothesis 6:** An increase in luggage divest time t_d and luggage collect time t_c result in a lower security throughput T_S .
- **Hypothesis 7:** An increase in luggage divest time t_d and luggage collect time t_c result a higher average contact time per passenger $C_{pax_{SL}}$ and $C_{pax_{SQ}}$.
- **Hypothesis 8:** Less luggage divest n_d and luggage collect n_c positions result in a lower average contact time per passenger $C_{pax_{SL}}$ and $C_{pax_{SQ}}$.

To test these hypotheses seven different scenarios were designed. In each scenario, only two security lanes are open. Passenger agents are generated in front of the queue of the security checkpoint. They only perform the queue activity and the security checkpoint activity. The inputs to the model for each scenario are given in Table 2. Scenario 1 is the baseline scenario with parameters simulating the pre-COVID19 situation, thus without any COVID-19 measures. Three luggage divest n_d and three luggage collect n_c positions are implemented per lane. Thus, passenger agents are standing there close to each other. Scenario 2 considers an increase of 20% in divest time t_d and collection time t_c . From interviews with airport stakeholders it was revealed that security operators do

not actively support passengers anymore during divesting which results in more time needed for passengers. When passengers place items incorrectly in the trays, operators try to minimize contact with the passengers' belongings. Therefore, they let passengers rather reorganize their items themselves which results in additional time. This scenario is used to test hypothesis 6 and 7. Scenario 4, 5, 6 and 7 consider different number divest n_d and collect positions n_c . Since the divesting and collection area is generally very crowded, pre-COVID-19 configurations with three divest positions and three collect positions per lane do not correspond to physical distance regulations any longer. These scenarios are used to test hypothesis 8.

Results for Security Check Point

Table 2 presents the results for this case study. In the baseline scenario, where the parameters from [19] were used, the throughput for the 2 lanes T_S is 230 passengers per hour. This is equal to 1.92 passengers per minute per lane, which is in line with the findings of [19]. As for the check-in case study, we observe from scenario 3 that physical distancing PD does not influence the security's throughput. Because the physical distancing is already analyzed in the previous case study, no further analysis is needed. For hypotheses 6 and 7, scenario 1 and 2 can be compared. In scenario 2, a 20% increase in divest t_d and collect t_c time was implemented (because operators do not actively support passengers to diminish the interactions). From Fig. 7, it was observed that most contacts happen at the luggage divest and collect area of the security system, therefore different number of luggage divest n_d and collect n_c positions were implemented.

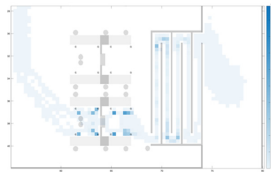


Fig. 7. Heatmap scenario 3. The dark blue areas represent the hot spots of passenger contacts. (Color figure online)

Table 2 shows that an increase in t_d and t_c has a negative influence on the throughput T_S . Throughput reduces by 10%. This reduction is supported by the coefficient of correlation $\rho_{t_d, T_S} = \rho_{t_c, T_S} = -0.51$ with a p -value of 0. Therefore hypothesis 6 can be supported. The average contact time per passenger at the security lane $C_{pax_{SL}}$ and in the queue $C_{pax_{SQ}}$ increased by around 13% and 15%. The coefficients of correlation are 0.42 and 0.39. Since this is lower than 0.4 (rule of thumb), we can't say there is a significant correlation. Therefore, we need to reject hypothesis 7. For hypothesis 8 we can compare scenario 4, 5, 6 and 7 in Table 2. Table 2 shows that a reduction in n_d and n_c lowers the average contact time per passenger at the security lane $C_{pax_{SL}}$. This correlation is confirmed by the coefficients: $\rho_{n_d, C_{pax_{SL}}} = 0.9$ and $\rho_{n_c, C_{pax_{SL}}} = 0.76$ (both with $p = 0$).

Table 2. Results of case study 2: security. PD means physical distancing, t_d luggage drop time, t_c luggage collect time, n_d number of divest positions per lane and n_c number of collect positions per lane. Note that percentages are given w.r.t. the baseline scenario 1.

Security scenario	Input to Model						T_S		C_{paxSL}		C_{paxSQ}	
	PD	t_d [sec]	t_c [sec]	n_d	n_c	μ [pax/h]	σ^2 [pax ² /h ²]	μ [min:sec]	σ^2 [sec ²]	μ [min:sec]	σ^2 [sec ²]	
1	No	N(54, 36)	N(71, 54)	3	3	230	15.9250	01:05	3.1485	01:52	4.9035	
2	No	N(65, 36)	N(85, 54)	3	3	206	-10% 12.9633	01:13	13% 2.9601	02:09	15% 3.2523	
3	Yes	N(65, 36)	N(85, 54)	3	3	206	-10% 15.0640	01:13	12% 4.9906	01:13	-35% 31.879	
4	Yes	N(65, 36)	N(85, 54)	2	3	165	-28% 13.8631	00:28	-57% 7.6131	01:36	-15% 68.954	
5	Yes	N(65, 36)	N(85, 54)	3	2	155	-33% 16.8833	00:59	-9% 7.9570	01:51	-1% 75.153	
6	Yes	N(65, 36)	N(85, 54)	2	2	137	-40% 10.1974	00:09	-86% 3.9940	02:01	8% 78.221	
7	Yes	N(65, 36)	N(85, 54)	1	1	69	-70% 17.7884	00:02	-97% 0.2418	04:20	132% 559.09	

Hypothesis 8 can be supported. However, Table 2 also shows that a reduction in n_d and n_c lowers the security throughput T_S . To find an optimal between the positive influence of n_d and n_c on the C_{pax} and the negative influence on T_S , some more analysis of the scenarios is needed: Comparing scenario 4 with scenario 5 shows that a “one divest position less” measure improves the C_{paxSL} better than “one collect position less”. From this, we can conclude in the luggage divest area more passenger contacts happen than in the collect area. Both measures have almost the same impact on security throughput T_S , around 160 passengers per hour. In scenario 6, one divest position less (scenario 4) and one collect position less (scenario 5) were implemented together. Table 2 shows that throughput reduces to 137 passengers per hour. The contact time at the security lane is reduced to 9 s per passenger, which means that almost no contacts occur at the security lane. Lastly, in scenario 7 only 1 divest position and 1 collect position per lane was implemented. For this scenario, the throughput T_S dropped even further to only 69 passengers per hour. The average contact time per passenger at the security lane dropped to 2 s per passenger while the contact time in the queue increased to 4 min and 20 s.

4.3 Case Study 3: Boarding

For case study 3, only boarding is considered. One gate area is considered and shown in Fig. 2. This case study aims to analyze the impact of the COVID-19 measures on the boarding procedure. For this case study, 50 passengers are considered representing a regional flight with a B737 with a load-factor of 1/3, based on expert knowledge. It is assumed that 50 passengers are all sitting at the start of the simulation. For this case study two metrics are considered, namely: 1. The average time to board 50 passengers T_B , calculated in minutes. Note: the time starts when the first passenger agent starts the boarding process (when the passenger agent leaves the seat) and it ends when the last (50th) passenger agent is boarded. 2. The average contact time per passenger C_{pax} , calculated in minutes. Using these metrics, four different hypotheses were found interesting to be analyzed:

- **Hypothesis 9:** Physical distancing increases the total time to board 50 passengers T_B .
- **Hypothesis 10:** Boarding in smaller groups increases the total time to board 50 passengers T_B .
- **Hypothesis 11:** Boarding in smaller groups decreases the average time passengers are in contact C_{pax} .

- **Hypothesis 12:** A higher average boarding pass check-time t_{bc} increases the average time passengers are in contact C_{pax} .

These hypotheses are tested by simulating four different scenarios. The inputs to the model for each scenario are given in Table 3. Scenario 1 is the baseline scenario in which passengers do not maintain physical distance, they board in groups of 10 and the t_{bc} follows a normal distribution with mean 10 s and variance 1 s. In scenario 2, passengers board in smaller groups of 5 passengers. This scenario is used to test hypotheses 10 and 11. In scenario 3 physical distancing is modelled to test hypothesis 9. Lastly, for hypothesis 12 scenario 4 simulates the impact of a higher t_{bc} because airlines often ask health questions before checking the boarding pass.

Results for Boarding

In case study, 3 different boarding strategies were analyzed. In total 5 scenarios were simulated. The results are shown in Table 3. For hypothesis 9, scenario 2 and 3 are compared. Scenario 2 in Table 3 shows that when passengers are not performing physical distancing PD , the time to board 50 passengers T_B is 4 min and 49 s. When passengers are performing physical distancing the time to board 50 passengers is 4% higher. This is also confirmed by the coefficient of correlation ρ_{PD, T_B} equal to 0.61 and the p-value equal to 0 which means there is a significant positive correlation. Thus hypothesis 9 can be supported. This makes sense because passengers need more time to organize themselves in the queue, especially at the beginning of the queue.

For hypotheses 10 and 11, scenario 1 and 2 are compared. Scenario 2 shows that when passengers are boarding in smaller groups GS (five passengers instead of ten) the time to board 50 passengers T_B increases by 12%. The average contact time per passenger C_{pax} decreases by 52%. This is also reflected by the coefficients of correlation which are $\rho_{GS, T_B} = -0.8$ (p-value of 0) and $\rho_{GS, C_{pax}} = 0.9$ (p-value of 0). Therefore hypothesis 10 and 11 can be supported. We can conclude that splitting a boarding group in two does not imply that the total boarding time doubles. This finding is important for airports with limited space at gates for queueing. Since some airlines ask additional questions related to COVID-19 during scanning of the boarding pass, passengers need to wait longer at the gate counter. Therefore, an increase of 10 s in boarding pass check time t_{bc} was implemented in scenario 4. To check hypothesis 12, scenario 3 and scenario 4 can be compared. Scenario 4 in Table 3 shows that an increase in boarding check time t_{bc} increases the average time a passenger is in contact C_{pax} with 4 s. The coefficient of correlation $\rho_{t_{bc}, C_{pax}} = 0.6$ with a p-value of 0. Therefore, hypothesis 12 can be supported. Moreover, it can also be seen from Table 3 that the total boarding time T_B significantly increases. Thus, the waiting time at the gate counter should be minimized as much as possible because it significantly influences the total boarding time and the average contact time per passenger. We can recommend that administrative questions should be asked in advance, for example, during online check-in.

Table 3. Results of case study 3: boarding. GS means boarding group size, PD means physical distancing and t_{bc} means boarding pass check time.

Boarding scenario	Input to Model			T_B		C_{pax}			
	GS	PD	t_{bc} [sec]	μ [min:sec]	σ^2 [sec ²]	μ [min:sec]	σ^2 [sec ²]		
1	10 pax	No	10	10:45		10.9984	01:04	1.1028	
2	5 pax	No	10	12:03	12%	21.5824	00:31	-52%	1.2914
3	5 pax	Yes	10	12:28	16%	24.4984	00:08	-88%	5.6517
4	5 pax	Yes	20	20:49	94%	25.3051	00:12	-81%	18.645
5	1 pax	Yes	20	34:25	220%	37.7517	00:00	-100%	0

5 Discussion and Conclusion

The proposed agent-based model simulates the main airport handling processes of passengers at an airport under COVID-19 circumstances. This study can help airport operators in their decision-making and make airports more resilient for future crises. The results from the three case studies are airport specific because the parameters used were specific to a particular regional airport. Data was taken from [16, 17] to calibrate the parameters for the case studies done with the model. As every airport has different distributions of passenger types and different infrastructure and personal, the used parameters can thus not per se be copied to represent other airports. Also, since there is not much work done in the field of agent-based models used for both the analysis of the airport operations performance and for the associated passenger health safety, it is difficult to compare the results with other studies. Although this study has proven to be useful in analyzing the impact of the COVID-19 measures, this study also made some assumptions. The contact time metric used in this research study takes into account distance (a contact happens when passengers are closer than 1.5 m from each other) and time (the time of a contact). However, the model does not distinguish between contacts that happen at 1 m and contacts that happen at 1.4 m. Lastly, the model only considers check-in desks staffed with operators. However, in reality many airports have self-check-in desks as these can spread over the passenger demand and decrease costs. This research study does not consider how self-check-in desks can contribute to safer operations for passengers.

This study aimed to analyze the impact of COVID-19 restrictions on airport operations' performance and the associated health safety of the passengers. The agent-based model was used to explore three different case studies to analyze the impact of these measures on the check-in, the security and the boarding process, respectively. The measures' effects were all tested in different scenarios for each case study by analyzing the maximum throughput and the average contact time per passenger for check-in and security. The results show that physical distancing during queueing does not affect the throughput of the check-in and the security process. Physical distancing does lead to passengers being less in contact with each other, and it also decreases the capacity of queues. The implementation of single queues instead of one common queue had a positive impact on the throughput of the check-in and the passengers' health safety. The flow towards desks is more efficient (with less interfering flows of passengers), and it is easier for physical distancing in single queues because no turning is required. Furthermore, it

was shown that in a pre-COVID-19 security lane set-up many passengers are too close at the luggage divest and collect area. The case study results showed that a decrease from three luggage divest and collect positions per lane to two positions of each per lane leads to a significant positive impact on passenger health safety while the throughput is still acceptable. However, to obtain the same throughput with one drop off and one collect position less it is advised to open an extra security lane. Implementing only one divest and one collect position per lane is unnecessary because it does not appropriately improve passenger health safety. Thus, two passengers per divest area and two per collect area is perfectly possible. Then, passengers can move without being closer than 1.5 m from each other. The boarding case study results showed that boarding in smaller groups positively impacts the average contact time per passenger. In contrast, it negatively affects the total boarding time. The results also showed that physical distance has a relatively small impact on the total boarding time because the organization of the passengers lining up during queuing takes a bit more time.

References

1. Covid19 airport status. <https://www.icao.int/safety/Pages/COVID-19-Airport-Status.aspx>. Accessed 14 Feb 2021
2. EASA: Covid-19 aviation health safety protocol - operational guidelines for the management of air passengers and aviation personnel in relation to the covid-19 pandemic. Technical report, European Union Aviation Safety Agency (2020)
3. De Herdt, C.: Massa mensen afgelopen weekend op luchthaven van Charleroi, viroloog Steven Van Gucht reageert verbaasd: Jammer dat dit gebeurt (2020). https://www.nieuwsblad.be/cnt/dmf20201221_98258870. Accessed 21 Mar 2021
4. Teknomo, K., Takeyama, Y., Inamura, H.: Review on microscopic pedestrian simulation model. arXiv e-prints [arXiv:1609.01808](https://arxiv.org/abs/1609.01808) (2016)
5. Gipps, P.G., Marksjö, B.: A micro-simulation model for pedestrian flows. *Math. Comput. Simul.* **27**(2), 95–105 (1985)
6. Blue, V., Adler, J.: Cellular automata microsimulation for modeling bidirectional pedestrian walkways. *Transp. Res. Part B Methodol.* **35**, 293–312 (2001)
7. Ma, W.: Agent-based model of passenger flows in airport terminals. Ph.D. thesis, Queensland University of Technology, Brisbane, Australia (2013)
8. Løvås, G.G.: Modeling and simulation of pedestrian traffic flow. *Transp. Res. Part B Methodol.* **28**(6), 429–443 (1994)
9. Okazaki, S., Matsushita, S.: A study of simulation model for pedestrian movement with evacuation and queuing. In: *Engineering for Crowd Safety*, p. 432 (1993)
10. Helbing, D., Farkas, I., Vicsek, T.: Simulating dynamical features of escape panic. *Nature* **407**(6803), 487–490 (2000)
11. Kierzkowski, A., Kisiel, T.: Simulation model of security control lane operation in the state of the COVID-19 epidemic. *J. Air Transp. Manag.* **88**, 101868 (2020)
12. Schultz, M., Soolaki, M.: Analytical approach to solve the problem of aircraft passenger boarding during the coronavirus pandemic. *Transp. Res. Part C: Emerg. Technol.* **124**, 102931 (2021)
13. Müller, S.A., Balmer, M., Neumann, A., Nagel, K.: Mobility traces and spreading of COVID-19, pp. 1–22. medRxiv (2020)
14. Ronchi, E., Lovreglio, R.: EXPOSED: an occupant exposure model for confined spaces to retrofit crowd models during a pandemic. *Saf. Sci.* **130**, 104834 (2020)

15. Janssen, S., Knol, A., Blok, A.-N.: AATOM - An Agent-based Airport Terminal Operations Model (2018). <http://stefjanssen.com/AATOMarchitecture.pdf>. Accessed 2021
16. Janssen, S., Sharpanskykh, A., Curran, R.: Agent-based modelling and analysis of security and efficiency in airport terminals. *Transp. Res. Part C Emerg. Technol.* **100**, 142–160 (2019)
17. Janssen, S., van der Sommen, R., Dilweg, A., Sharpanskykh, A.: Data-driven analysis of airport security checkpoint operations. *Aerospace* **7**(6), 69 (2020)